Engineering and Technology Journal
Journal homepage: https://etj.uotechnology.edu.iq

Integrating Grey Relation Analysis and Artificial Neural Networks for Optimal Machining of Tungsten Carbide Composite Using Hybrid Electrochemical Discharge

Vian N. Najm*, **Tahseen F. Abbas**, **Shukry H. Aghdeab**

Production Engineering and Metallurgy Dept., University of Technology-Iraq, Alsina'a street, 10066 Baghdad, Iraq.
*Corresponding author Email: vian.n.najm@uotechnology.edu.iq

HIGHLIGHTS

- This study implements the machining of tungsten carbide using hybrid electrochemical discharge machining
- Grey relation analysis (GRA) and artificial neural network (ANN) approaches are utilized for optimization
- The maximum material removal rate and highest machining depth are attained by applying the optimum parameters
- The electrolyte concentration affects material removal rate and machining depth most, followed by current.

ARTICLE INFO

Handling editor: Omar Hassoon

Keywords:

Electrochemical discharge machining (ECDM); material removal rate (MRR); depth of cut (DOC); grey relation analysis (GRA); artificial neural network (ANN).

ABSTRACT

Hybrid Electrochemical Discharge Machining (ECDM) streamlines the manufacturing process for challenging materials. Tungsten carbide (WC) is widely recognized as a formidable material due to its exceptional hardness and its ability to maintain hardness even at elevated temperatures. This study has conducted a comprehensive investigation of the multi-response optimization of ECDM process parameters to enhance the machining of tungsten carbides, utilizing Grey Relation Analysis (GRA) and Artificial Neural Network (ANN) methods. This optimization's primary objective is to achieve the maximum Material Removal Rate (MRR) and machining depth. The study involved a systematically designed experiment based on the Taguchi design method. Scanning Electron Microscopy (SEM) analysis reveals shallow craters, minimal microcracks, and small melt re-deposits on the machined surfaces, elucidating the smooth surface achieved after ECD machining. The average surface roughness achieved in this study, utilizing Electrochemical Discharge Machining (ECDM) for tungsten, measured at 0.9275 µm. Optimal parameters were determined, including a current of 80 A, a stand-off distance of 0.1 mm, a 30 mm gap, and an electrolyte composed of KCl + KOH for machining tungsten carbide. The results of the Analysis of Variance (ANOVA) indicate that electrolyte concentration has the most significant impact on machining depth and material removal rate (50.55%), followed by the current value (31.32%). Additionally, the ANN results aligned closely with those obtained through GRA. Compositional analysis of the surface using Energy-Dispersive X-ray Spectroscopy (EDS) mapping confirms the presence of oxides and carbon on the machined surface.

1. Introduction

Electrochemical Discharge Machining (ECDM) is an economically viable and versatile non-conventional machining technique commonly used to manufacture conductive and non-conductive materials [1]. The ECDM method is a hybrid manufacturing technique that integrates the principles of Electrical Discharge Machining (EDM) and Electrochemical Machining (ECM) to enhance product production efficiency [2]. One notable benefit of Electrochemical Discharge Machining (ECDM) compared to Electrochemical Machining (ECM) or Electrical Discharge Machining (EDM) is the combination of multiple metal removal processes, resulting in a significantly increased machining rate [3]. This method can manufacture electrically conductive materials much faster, ranging from five to fifty times faster than traditional ECM and EDM methods [4].

Tungsten carbide (WC) and its composites have widespread applications in the industrial world [5]. The problem arises from the inherent challenges associated with machining tungsten carbide, a material renowned for its distinctive chemical and physical properties and exceptionally high melting point of 2,870 degrees Celsius [6]. Therefore, non-traditional machining processes such as Electrical Discharge Machining (EDM) and Electrochemical Machining (ECM) are used for machining tungsten carbides. In the EDM process, the high temperature of the spark and electrode causes wear on the electrode [7]. In the ECM process, material is removed through the anodic dissolution of the workpiece [8]. Several studies have been conducted to enhance

http://doi.org/10.30684/etj.2023.143347.1581
Received 19 September 2023; Received in revised form 11 October 2023; Accepted 04 November 2023; Available online 08 December 2023
2412-0758/University of Technology-Iraq, Baghdad, Iraq

the machining of WC. Among these studies, Kumar et al. [9], tried to determine an optimal technique for cutting tungsten carbide by manipulating various parameters within the EDM (Electrical Discharge Machining) process. The primary objective is achieving the highest possible Material Removal Rate (MRR) while improving surface finish. Janmanee and Kumjing [6], established an Artificial Neural Network (ANN) model to predict microcracking during Electrical Discharge Machining (EDM) of tungsten carbide (WC-Co) composite materials.

However, there are limitations to electrical discharge machining (EDM) [10]. Excessive tool wear, the production of recast layers, and geometrical inaccuracy are further issues associated with EDM [11]. The characteristics of the recast layer differ from those of the starting material principally due to the effects of heat treatment and quenching, which are commonly regarded as limitations of the process [12]. The crater's features are influenced by either the redeposition of molten debris or their efficient removal, which significantly impacts the occurrence of arcing. A debris layer trapped within the interaction zone reduces the intensity of the sparks [13]. Researchers made many efforts to enhance the material removal rate by reducing the limitations of electrochemical discharge machining. Rafaqat et al., [14]. With the development of a novel, unconventional electrode and the application of electrical discharge machining on D2 steel using copper as the electrode material, substantial enhancements were realized. These included an approximate 70% increase in material removal rate, a reduction in tool wear rate by about 45-50%, and a nearly 10% decrease in the taper angle.

Farooq et al. [15] used grey relational analysis to confirm reduced process limitations. This reduction was substantiated through experimental results, which demonstrated values of 0.109 mm for spark gap, 0.956% for angular deviation, 3.49% for radial deviation, and 2.2 μm for surface roughness. Additionally, they introduced an innovative flushing mechanism that led to a 1.92% enhancement in spark gap and notable reductions in angular and radial deviations by 8.24% and 29.11%, respectively. Naoki et al. [16], presented the manufacturing of micro-pins made from a tungsten carbide (WC) alloy using the electrochemical machining (ECM) technique. The investigation focuses on machining conditions, utilizing a neutral electrolyte solution of $NaNO_3$ in an aqueous medium. However, the ECM method also has its drawbacks. Since a customized tool must be designed for each unique component geometry, ECM is typically only cost-effective for mass manufacturing. Disposing of the process electrolyte can be problematic if it has accumulated heavy elements like chromium or cadmium [17].

To advance technology and overcome the primary limitations of these procedures, hybrid machining techniques that combine two or more of these approaches have been developed [18]. Sathisha et al. [19], created an experimental setup for Electro Chemical Spark Machining (ECSM) to machine soda-lime glass. Grey relational analysis was employed to optimize process parameters associated with various responses, including the Material Removal Rate (MRR) and Tool Wear Rate (TWR). The effects of process variables on material removal and tool wear, such as tool-to-workpiece distance, applied voltage, and electrolyte concentration, were investigated. Additionally, Analysis of Variance (ANOVA) was utilized to determine which variables had the greatest impact on both the Material Removal Rate (MRR) and the Tool Wear Rate (TWR). Durairaja et al. [20], have described the Grey Relational Theory and Taguchi optimization approach, which were employed to determine the optimal settings for Wire EDM cutting of SS304. This optimization's primary objective is to maximize kerf width (the thickness of the cut) and surface quality (the smoothness of the finished product).

The research involves using a stainless steel 304 workpiece, with optimization inputs including gap voltage, wire feed, pulse on time, and pulse off time. The ideal kerf width and surface roughness values are independently determined using the Taguchi optimization method. Additionally, Analysis of Variance (ANOVA) is a valuable tool for identifying the most influential variable. Manikandan et al. [21], studied the Electrochemical Machining (ECM) of Inconel 625 material using the Grey Relational Analysis (GRA) approach. Three input machining variables were investigated, namely feed rate, electrolyte flow rate, and electrolyte concentration. In addition to material removal rate and surface roughness, geometric measures such as overcut, form, and orientation tolerance were included as performance measures in this investigation. The analysis results indicate that the feed rate is the predominant variable influencing the desired performance characteristics. Based on the established performance measures, multiple regression models were developed for use as predictive tools. Kumar et al. [22], utilized Grey Relational Analysis (GRA) to determine the optimal values for output parameters in electrochemical discharge machining, specifically material removal rate (MRR) and hole taper angle (HTA).

The objective of this research was to investigate the effects of varying the electrolyte content, voltage, and duty factor on a micro hole drilled into a piece of Ti-6Al-4V. Throughout the planning and testing phases, the orthogonal array L9 was employed. The results indicate that voltage is the most influential factor for both MRR and HTA, followed by electrolyte concentration and duty factor. This approach yielded a maximum mass transfer rate of 1.50 mg/min and a minimal taper angle of 0.98°. According to GRA, the optimal machining conditions involve an electrolyte concentration of 3M, a voltage of 40 V, and a duty factor of 25% . At the same time, Pravin Pawar et al. [23] used grey relational analysis optimization to find the best combination of inputs to achieve a desired output while milling silicon carbide on a home-built ECDM machine employing gunmetal cutting tools. Taguchi's L27 orthogonal array method was utilized in the experiments. Following the drilling of silicon carbide material, input process parameters, including electrolyte concentration, applied voltage, and tool rotation, were examined, as were the outcomes, including machined depth and hole diameter. The data showed electrolyte concentration is more critical than voltage and tool rotation in determining the drilled hole's diameter and depth [23]. Based on the literature review above, the paper highlights the versatility of the grey relation method in various machining processes and materials, reliably delivering favorable results and being easy to grasp. The paper introduces the GRG method for assessing the impact of various parameters in electrochemical discharge machining (ECDM) on the grey relational coefficients of material removal rate (MRR) and machining depth (MD) when working with tungsten carbide workpieces. This integration allows for the simultaneous treatment of multiple objectives. Tungsten carbide materials maintain high hardness levels and modulus of elasticity even under high heat. This research explores methods to enhance the productivity of the ECDM process for tungsten carbides. This study contributes significantly by utilizing a multi-response grey relation analysis combined with an artificial neural network strategy to improve electrochemical discharge

machining performance, particularly concerning material removal rate and depth of cut, on the challenging tungsten carbide material.

2. Methodology

2.1 Material Selection

Tungsten carbides find use where other materials would wear out too rapidly or break down entirely. Their high levels of hardness and strength are one of their defining characteristics [16]. Tungsten carbide (WC) and its composites find numerous industrial applications, such as wear-resistant parts in hot rolling mills and drawing dies, mining and cutting tools, precise drilling tips, and sandblast nozzles [5]. This study chose tungsten carbide inserts as the workpiece material, representing this challenging material due to their exceptional hardness and toughness. Figure 1 shows the WC workpiece before machining.

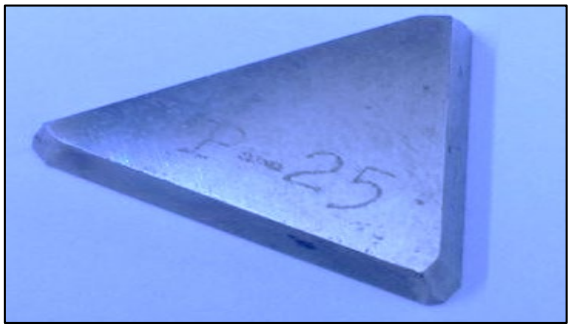

Figure 1: Tungsten carbide workpiece before machining

2.2 Experimental Set Up

An experimental apparatus for ECDM was designed. Figure 2 shows a schematic diagram of the ECDM experimental apparatus. A pulse direct current (DC) power source was developed for experimental purposes, allowing for variable current adjustments while maintaining constant voltage. The power supply's standard current output can be adjusted from 20 A to 100 A. The workpiece is immersed and secured by a fixture inside the solution tank, as shown in Figure 3, made of acrylic and sized at 440×200×80 mm³.

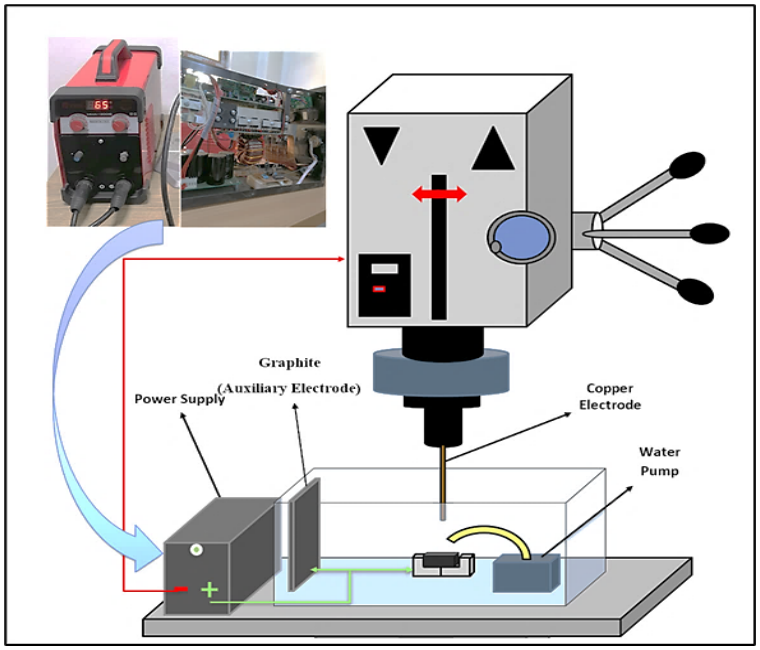

Figure 2: A schematic diagram of the ECDM experimental apparatus design with modifications inside the power supply

Figure 3: The workpiece is immersed in the solution tank, copper electrode, and aluminum workpiece holder

A tool electrode with a copper composition and a 10 mm radius is partially submerged in the electrolyte, maintaining a fixed distance for spark generation. Copper was chosen as the tool electrode due to its excellent erosion resistance and high electrical conductivity. Graphite was selected as the auxiliary electrode for its high resistance to electrolytes and chemical inertness. The flow chart of the research methodology has been assigned in Figure 4.

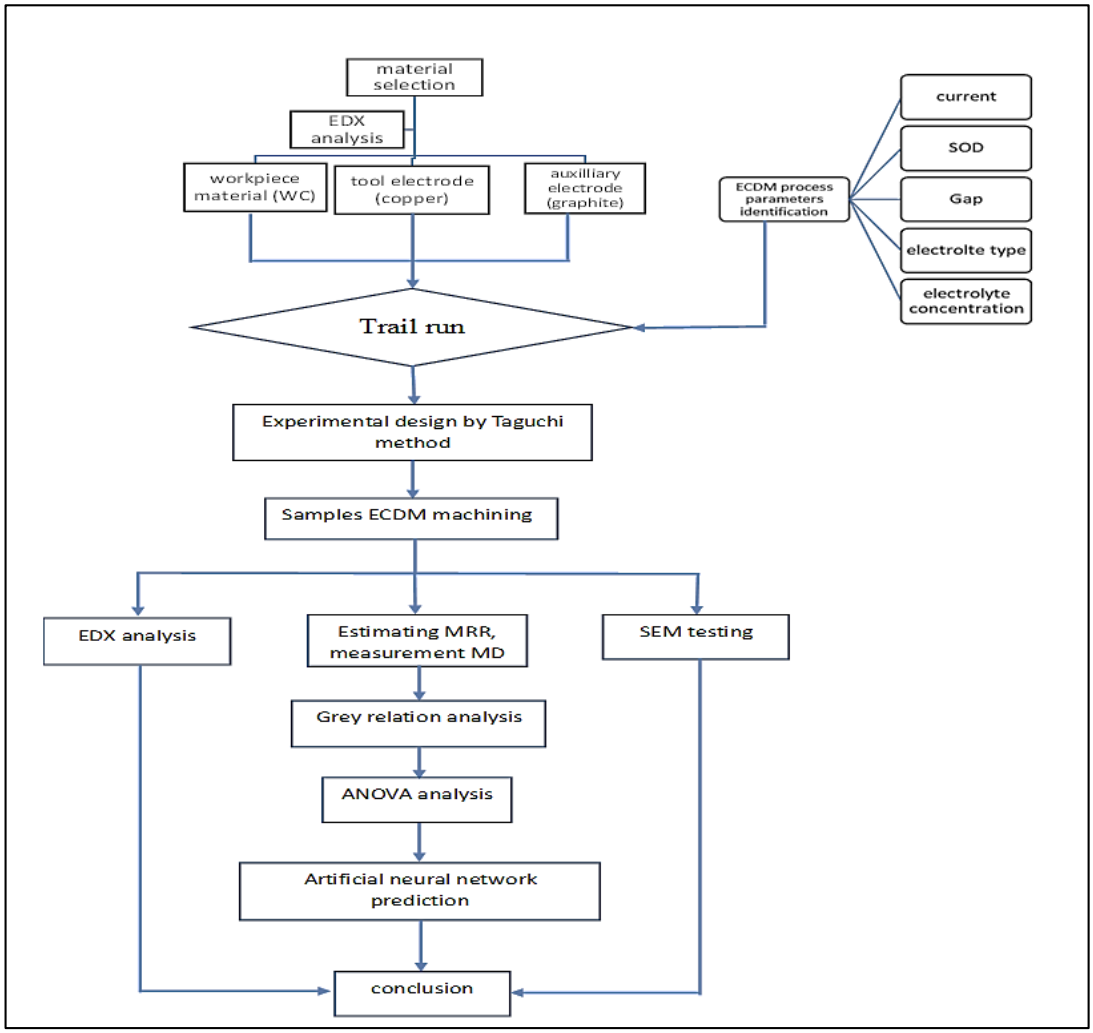

Figure 4: Flow chart of research methodology

2.3 Characterization

The chemical composition of the tungsten carbide workpiece and copper electrode was analyzed using energy-dispersive X-ray spectroscopy at the Alkhora Company's NANO Research SEM Laboratory. Table 1 presents the chemical composition of tungsten carbides, while Table 2 displays the chemical composition of the copper electrode. Figure 5 shows the copper electrode used in the experiments.

Table 1: Chemical composition of the workpieces used before machining.

Element	Atomic %	Atomic % Error	Weight %	Weight % Error
C	71.7	0.7	19.4	0.2
Ca	0.1	0.0	0.1	0.0
Ti	4.8	0.1	5.1	0.1
Cr	0.4	0.0	0.5	0.1
Fe	1.5	0.1	1.9	0.1
Co	4.1	0.1	5.5	0.1
Ni	1.5	0.1	2.0	0.1
W	15.9	0.1	65.6	0.5

Table 2: Chemical composition of copper electrode

Element	Atomic %	Atomic % Error	Weight %	Weight % Error
C	44.3	0.8	16.0	0.3
O	14.1	0.3	6.8	0.2
Al	0.4	0.1	0.3	0.1
Si	1.0	0.1	0.8	0.0
S	0.1	0.0	0.1	0.0
Cl	0.4	0.0	0.4	0.0
Ca	0.2	0.0	0.3	0.0
Cu	39.5	0.2	75.3	0.4

Figure 5: The copper electrode used in the experiments

2.4 Experimental Design and Data Collection

The present study examined various process parameters on tungsten carbide workpiece material to determine the optimal conditions for creating a gas film around the tool, thus facilitating the machining process through etching. The Taguchi design method was employed for experimentation, involving five parameters tested at five levels each. The fractional factorial design used was a standard L5 (5^5) orthogonal array, as depicted in Table 3 below, along with the output variables.

The electrolytes are denoted by numbers, as shown in Table 4 below. The remaining process parameters were fixed, as shown in Table 5 below.

Table 3: Designed ECDM process parameters using Taguchi method

No.	Current (Amp)	SOD (mm)	Gap (mm)	Electrolyte	Concentration (%)
1	20	0.1	30	1	0.05
2	20	0.2	40	2	0.10
3	20	0.3	50	3	0.15
4	20	0.4	60	4	0.20
5	20	0.5	70	5	0.25
6	35	0.1	40	3	0.20
7	35	0.2	50	4	0.25
8	35	0.3	60	5	0.05
9	35	0.4	70	1	0.10
10	35	0.5	30	2	0.15
11	50	0.1	50	5	0.10
12	50	0.2	60	1	0.15
13	50	0.3	70	2	0.20
14	50	0.4	30	3	0.25
15	50	0.5	40	4	0.05
16	65	0.1	60	2	0.25
17	65	0.2	70	3	0.05
18	65	0.3	30	4	0.10
19	65	0.4	40	5	0.15
20	65	0.5	50	1	0.20
21	80	0.1	70	4	0.15
22	80	0.2	30	5	0.20
23	80	0.3	40	1	0.25
24	80	0.4	50	2	0.05
25	80	0.5	60	3	0.10

Table 4: Electrolytes selected for ECDM process

Type of electrolyte	NO
KCl	1
NaCl	2
NaCl+NaOH	3
KCl +KOH	4
NaCl + KCl +KOH+NaOH	5

Table 5: ECDM process fixed parameters

Parameters	Descriptions
Workpiece material	Tungsten Carbide
Tool electrode	Copper
Auxiliary electrode	Graphite
Voltage	70 volt
Machining time	15 min

3. Material Removal Rate and Machining Depth

Considering the significance of the material removal rate (MRR) and the depth of cut (DC) as evaluation metrics for assessing the effectiveness of the ECDM process, tests were conducted to investigate the impact of ECDM process parameters on MRR and DC. A digital balance was employed to weigh the workpiece both before and after the operation to determine the weight difference, with a measurement range of (0.01-220) grams, ensuring precision with an accuracy of (±0.0003). The material removal rate was calculated using Equation 1, while the depth of cut was measured using a high-precision micrometer with a resolution of 0.01 mm.

$$MRR = \frac{wieght\ before - wieght\ after}{machining\ time} \tag{1}$$

4. Theoretical Part of The Grey Relation Method

Grey system theory effectively manages ambiguity, complexity, and knowledge gaps. The Grey Relational Analysis (GRA) method evaluates the precise connections between sequences by quantifying their total information variation [21]. GRA is a technique for elucidating connections among multiple responses. The steps of grey relational analysis are outlined below with supporting references [24,19,25]:

The first step is to determine the S/N ratio for each category, which was determined as follows:

(For larger is better)

$$\left(\frac{S}{N}\text{ratio}\right) = -10\ \text{Log}\left(\frac{1}{n}\right)\sum_{k=1}^{n} {}^{1}\!/_{x_{kj}^2} \tag{2}$$

(For smaller is better)

$$\left(\frac{S}{N}ratio\right) = -10\ Log\left(\frac{1}{n}\right)\sum_{k=1}^{n} x_{kj}^2 \tag{3}$$

where n is the number of repetitions, X is the detected response value, k ranges from 1 to n, and j ranges from 1 to k. This method is of utmost importance when optimizing a critical quality parameter [24].

The second step is Normalizing the original data before analysis, whether with the grey connection theory or any other methodology, eliminates the impact of using different units and reduces variability [24], which normalizes outputs in the range (0 to 1) [20]. For larger is better, the following formula is used:

$$y_i(k) = \frac{x_i^0\ (k) - \min x_i^0(k)}{\max x_i^0(k) - \min x_i^o(k)} \tag{4}$$

(For smaller is better)

$$y_i(k) = \frac{max\ x_i^0\ (k) - x_i^0(k)}{\max x_i^0(k) - \min x_i^o(k)} \tag{5}$$

where i represents the test number, ranging from 1 to 25; k denotes the k-th performance characteristic; x_i^0 (k) is normalized as y_i (k) ($0 \le y_i \le 1$) [24,23].

The third step is an estimation of the grey relational co-efficient for the normalized S/N ratio values.

$$\Sigma i\ (k) = (\Delta min + \Sigma\Delta max)/(\Delta oj + \Sigma\Delta max) \tag{6}$$

where $\Sigma i\ (k) =$ grey relation grade and Δmin in this study equals 0, and Δmax equals 1. ε is a positive number between 0 and 1. The value of ε can be adjusted to meet the requirements of the service users, with a smaller value indicating better distinguishing ability. This study set ε to 0.5 [24, 26].

The fourth step is the generation of the grey relational grade, which assigns a grade to each of the coefficients to rank the experiments.

$$\gamma = 1/n\ \sum_{k=1}^{n} \Sigma\text{i (k)} \tag{7}$$

where γ is the grey relational grade, n represents the number of output characteristics (n = 2 in this study). The outcomes of the grey relational analysis are derived based on these parameters [24,23].

5. Results and Discussion

We will discuss the results obtained in this sector using grey relational analysis with artificial neural networks. Analysis of variance is employed to predict the impact of machining parameters on the grey relational grade. After conducting the experiments outlined in Table 3, Equation 1 defines the material removal rate (MRR) as the ratio of the difference in weight of the machined item before and after machining to the machining time. Additionally, the mean deviation (MD) was measured, and the experimental results from these trials are presented in Table 6 below. Figure 6 illustrates the workpiece after machining.

Table 6: MRR and MD values obtained from the experiments

NO	MRR (g/min)	MD (mm)
1	0.04422	0.34
2	0.04316	0.33
3	0.05066	0.39
4	0.05784	0.43
5	0.06122	0.45
6	0.07152	0.55
7	0.07760	0.61
8	0.04116	0.32
9	0.04076	0.29
10	0.05194	0.38
11	0.05814	0.47
12	0.05842	0.45
13	0.06020	0.44
14	0.07936	0.61
15	0.04696	0.37
16	0.08306	0.63
17	0.05074	0.42
18	0.06552	0.52
19	0.06400	0.50
20	0.06600	0.48
21	0.07770	0.60
22	0.08950	0.70
23	0.09250	0.71
24	0.05280	0.40
25	0.05990	0.45

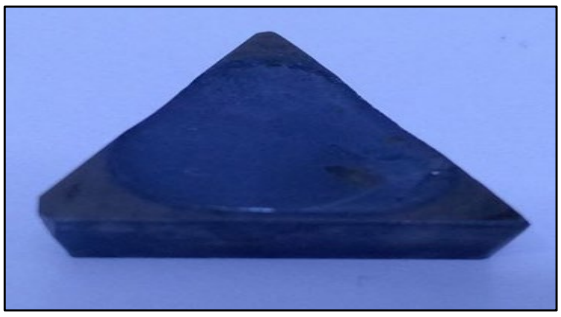

Figure 6: Tungsten carbide workpiece after machining

5.1 Grey Relational Analysis

The first step is determining the S/N ratio for the material removal rate and machining depth as output responses. In this work, the "larger is better" formula has been used [26]. In this case, the preference for a larger formula is justified by the primary objective of achieving a higher material removal rate, especially through increased depth, using Equation 2.

In the case of this specific level of difficulty, the larger the response value, the better [24]. Table 7 shows the S/N ratio for MRR and MD. The estimate of signal-to-noise ratio values was conducted with a single repeat, where n = 1.

The second step: The normalization method's sensitivity has also been investigated on the sequencing findings, considering its impact on the rank. The findings indicate that using the S/N (signal-to-noise) value for data normalization in grey connection analysis is recommended. Regarding performance, the preprocessing of metal removal rate data can be characterized using Equation 4 and illustrated in Table 7.

The third step of the grey relational co-efficient for the normalized S/N ratio for each level of the experiments has been estimated values using Equation 6, the grey relation coefficient values shown in Table 8. The grey relation coefficient is considered an entrance for estimating the grey relation grade.

The fourth step involves generating the grey relational grade using Equation 7, which assigns a grade to each of the coefficients of the grey relation, as shown in Table 8. The final step is to rank the experiments in Table 8 based on the grade relation values obtained in the previous step. The optimal combination of process parameters, resulting in the highest material removal rate and machining depth, was found in experiments 23, 22, and 16. Conversely, experiments 9, 8, and 2 yielded the

lowest material removal rate and machining depth. It can be concluded that the higher grey relational grade indicates a higher quality product.

Table 7: S/N Ratio values for the corresponding responses and Normalized S/N ratio values

NO	S/N Ratio		Normalized values	
	MRR	MD	MRR	MD
1	-27.08762524	-9.370421659	0.099420656	0.177649686
2	-27.29837128	-9.629721202	0.069813805	0.144308726
3	-25.90669629	-8.178707859	0.265324543	0.330881276
4	-24.75543431	-7.330630888	0.427060639	0.439927746
5	-24.26213349	-6.935749724	0.496362458	0.490701907
6	-22.91144988	-5.19274621	0.686114485	0.714818806
7	-22.20276557	-4.2934033	0.785674651	0.830457095
8	-27.71049268	-9.897000434	0.011916552	0.109941732
9	-27.79531649	-10.75204004	0	0
10	-25.68996109	-8.404328068	0.295772786	0.301870835
11	-24.71049945	-6.558042841	0.433373355	0.539267785
12	-24.66876895	-6.935749724	0.439235903	0.490701907
13	-24.40807017	-7.13094647	0.475860409	0.465603341
14	-22.00796682	-4.2934033	0.813041133	0.830457095
15	-26.56543824	-8.635965519	0.172780576	0.272086691
16	-21.61216146	-4.013189011	0.868646212	0.86648729
17	-25.89299074	-7.535014192	0.26724998	0.413647964
18	-23.67252222	-5.679933127	0.579194538	0.652175891
19	-23.87640052	-6.020599913	0.550552509	0.608372661
20	-23.60912129	-6.375175252	0.588101477	0.562781058
21	-22.19157962	-4.436974992	0.787246119	0.811996522
22	-20.96353929	-3.0980392	0.959768493	0.984158044
23	-20.67716535	-2.974833026	1	1
24	-25.54732155	-7.958800173	0.315811634	0.359157196
25	-24.45146355	-6.935749724	0.469764251	0.490701907

Table 8: Grey relation coefficient and grey grade values with ranking

NO	Grey relation coefficient		grade	Rank
	MRR	MD		
1	0.356995126	0.37811463	0.367554878	22
2	0.349604829	0.368815533	0.359210181	23
3	0.404964719	0.427672562	0.416318641	19
4	0.466009561	0.471665963	0.468837762	16
5	0.498187821	0.495393783	0.496790802	11
6	0.614337018	0.63679569	0.625566354	7
7	0.69996116	0.746778132	0.723369646	5
8	0.336002662	0.359697152	0.347849907	24
9	0.333333333	0.333333333	0.333333333	25
10	0.415204037	0.417317276	0.416260656	20
11	0.468767588	0.520436384	0.494601986	12
12	0.471358336	0.495393783	0.48337606	15
13	0.488214697	0.483373564	0.485794131	14
14	0.727845617	0.746778132	0.737311874	4
15	0.376727458	0.40719487	0.391961164	21
16	0.791948998	0.789250148	0.790599573	3
17	0.405597235	0.460255961	0.432926598	17
18	0.543002861	0.589744966	0.566373913	8
19	0.526622067	0.560772397	0.543697232	9
20	0.548306623	0.533493272	0.540899948	10
21	0.701504423	0.726740512	0.714122468	6
22	0.925529136	0.969289128	0.947409132	2
23	1	1	1	1
24	0.422230123	0.438272476	0.4302513	18
25	0.485325811	0.495393783	0.490359797	13

5.2 ANOVA for Grey Relational Analysis

The optimal factor and its level combination are determined subsequently using ANOVA analysis. Since a higher grey relational grade indicates a higher quality product, this grade can be utilized to estimate the factor effect and identify the optimum value for each controllable variable [24,27].

The grey relational grade chart for the levels of the processing parameters is depicted in Figure 7. A higher grey relational grade indicates better performance across multiple output characteristics. However, to effectively determine the optimal

combinations of the method parameter levels, the absolute value of the parameters for different output characteristics must be known [24]. Table 9 describes and presents the mean of the grey relational grade for each parameter level. The (*) symbol indicates the highest grade value for each parameter. The optimum levels for maximum grade were current at level five, stand-off distance at level one, Gap at level one, and electrolyte at level four, with concentration at level five.

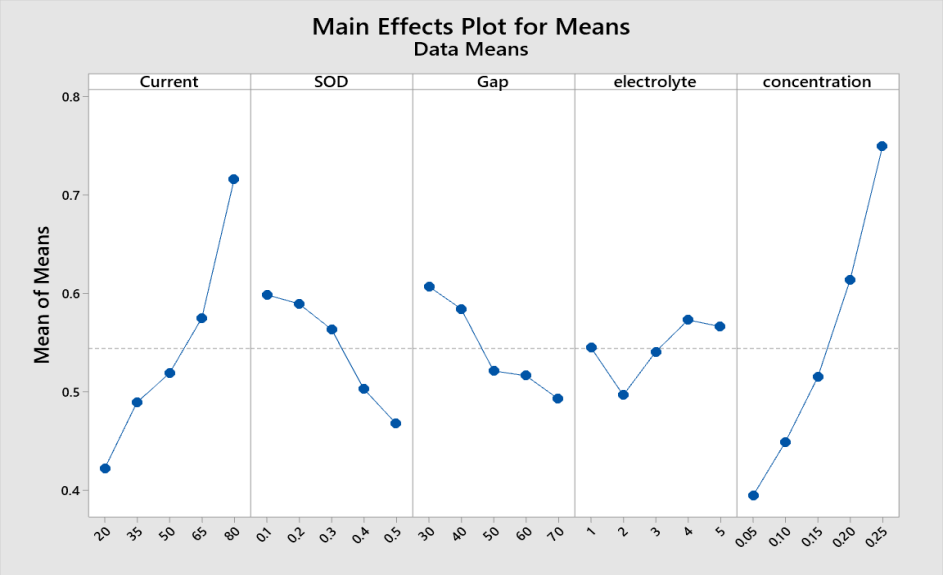

Figure 7: Main effects chart of the processing parameters on the grey relational grade

Table 9: Response Table for Means of grey relational grade

Level	Current	SOD	Gap	Electrolyte	Concentration
1	0.4217	0.5985*	0.6070*	0.5450	0.3941
2	0.4893	0.5893	0.5841	0.4964	0.4488
3	0.5186	0.5633	0.5211	0.5405	0.5148
4	0.5749	0.5027	0.5162	0.5729*	0.6137
5	0.7164*	0.4673	0.4926	0.5661	0.7496*
Delta	0.2947	0.1312	0.1144	0.0765	0.3555
Rank	2	3	4	5	1

After identifying the significant factors through ANOVA (analysis of variance), the analysis aims to determine which process factors of the linear motion guide significantly impact the performance characteristics [19]. A bigger proportion of contribution indicates a more significant impact on the features of the final product [28]. The results of the ANOVA for the Grey relational grade and the relative contributions of each operational variable are displayed in Table 10. ANOVA was employed to evaluate the null hypotheses of the observed data at a 95% confidence level ($\alpha = 0.05$) to ascertain the statistical significance. Parametric significance is ascertained by comparing P-values with the confidence level (α). If the P-value is less than or equal to α (P-value $\leq \alpha$), it indicates a statistically significant difference in the mean values of the specific parameter.

Conversely, if the P-value is greater than α (P-value $> \alpha$), it suggests there is no statistical significance among the mean values [29]. Considering the impact of individual parameters (P-value < 0.05), the analysis of variance underscores that the electrolyte concentration and current have the most significant effects. Specifically, the data indicates that the electrolyte concentration contributes 50.55%, while the current contributes 31.32%. In this context, (DF) represents degrees of freedom, (SS) represents the sum of squares, (MS) represents the mean square value, and a higher value of the (F-test) indicates a more significant factor. The contribution percentage of individual parameters can be determined from the ANOVA Table 10 using the following expression.

$$\text{Percentage contribution (PC\%)} = \frac{Sum\ of\ Square\ of\ Variation}{Total\ Sum\ of\ Square\ of\ Variation} * 100\% \quad (7)$$

Table 10: Analysis of Variance outcomes

Source	DF	Adj SS	Adj MS	F-Value	P-Value	PC%
Current	4	0.24636	0.061591	20.45	0.006	31.32
SOD	4	0.06493	0.016231	5.39	0.066	8.26
Gap	4	0.04757	0.011892	3.95	0.106	6.05
Electrolyte	4	0.01800	0.004501	1.49	0.353	2.29
Concentration	4	0.39763	0.099407	33.00	0.003	50.55
Error	4	0.01205	0.003012			1.53
Total	24	0.78654				100

From the main effect plot chart in Figure 7, it is evident that the optimal parameter levels include a current of 80 A, a Stand-off Distance (SOD) of 0.1 mm, a gap of 30 mm, an electrolyte composed of (KCl + KOH), and a concentration of 25%. These parameters lead to the maximum material removal rate and greater machining depth. The confirmation test results using these optimal machining parameters produce consistent outcomes. The grey relation analysis and ANOVA outcomes reveal that the higher current and electrolyte concentration level produces maximum MRR and MD. This happens because the rising current and concentration result in more hydrogen bubbles forming between the two electrodes, subsequently increasing the voltage. Consequently, these bubbles are more likely to reach the breakdown voltage and initiate sparking [30]. Also, the current values' enhancement leads to rising discharge energy. The following Equation shows the relation between the mean discharge energy and current.

$$E = V \times I_{dis} \times t \quad (8)$$

where, E =Energy of discharge (Joule), V =Critical voltage (V), I_{dis} =Mean discharge current (A), t =Mean discharge interval (t) [31]. The discharge energy is then converted into thermal energy, increasing temperature. This elevated temperature leads to localized melting and evaporation of the workpiece material. While the gap between the workpiece and the tool electrode plays a significant role, in conclusion, in ECDM, the space between the tool electrode and the workpiece affects the equilibrium between sparks and anodic dissolution. Smaller gaps promote spark actions, while larger gaps promote electrochemical dissolution [32]. Electrochemical discharge machining (ECM) operations are exclusively observed at greater gaps, resulting in a limited material removal rate (MRR).

Also, the results show that advanced material removal rate and machining depth values were obtained at the lowest stand-off distance value. As the SOD increases, the kinetics of electrochemical reactions diminishes, resulting in a decrease of sparking phenomenon[33]. Further elaboration reveals that the stability of the gas film experiences a rise in direct proportion to the augmentation of the distance between the electrodes. The observed phenomenon may be attributed to the rise in electrochemical resistance, directly proportional to the increase in the spatial separation between the electrodes. The phenomenon above leads to a decrease in electrochemical activity, reducing the volume of the gas film. Consequently, the buoyant force is ultimately diminished. This phenomenon enhances gas film stability, resulting in minor energy discharges [34].

5.3 Artificial Neural Network

One of the most widely used predictive model types, Artificial Neural Networks (ANNs), can estimate the outputs of machining operations across a broad spectrum of input parameters [35]. In this research, an Artificial Neural Network (ANN) is represented as a network of interconnected neurons using ad hoc linkages. The feed-forward neural network with backpropagation is considered the most versatile among various types of neural networks. The network consists of five inputs, including current, stand-off distance, gap, electrolyte concentration, and type, with one output representing the grey relational grade. The ANN was trained using the Neural Network Toolbox in the MATLAB environment. A feed-forward neural network with a single hidden layer containing ten neurons was determined to perform the best. The diagram of the artificial neural network model created with the Pattern Recognition Tool is shown in Figure 8. The network structure 5-10-1, which achieved the lowest mean absolute prediction error of 0.0005, was considered the optimal choice for this study, as depicted in Figure 9. A strong correlation was established between the experimental output and the network output, as indicated by the validation data set regression coefficient (R) of 0.99769, which is close to 1.

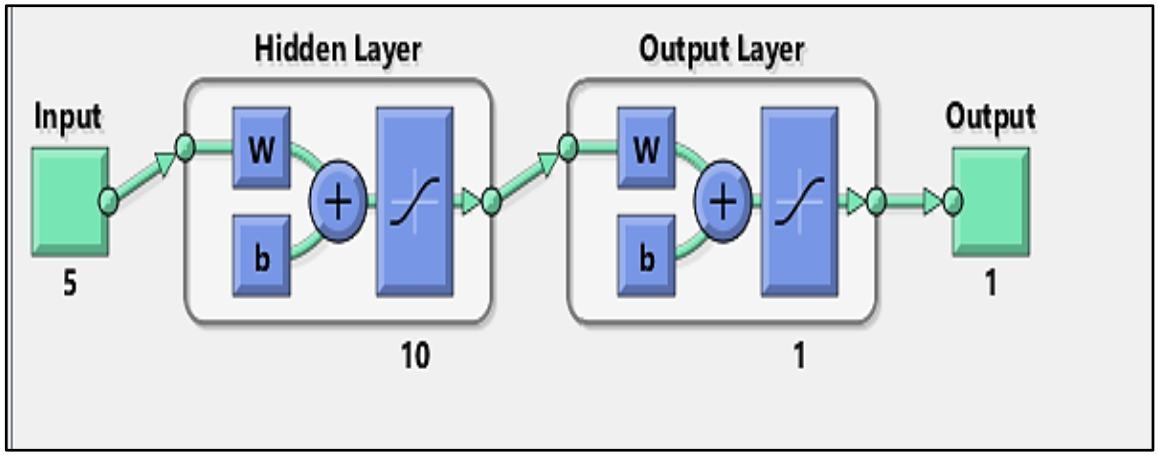

Figure 8: Diagram of artificial neural network model created with the Pattern Recognition Tool

In the context of supervised training, the dataset is typically partitioned into three distinct groups, as shown in Figure 9, the training set, the validation or verification set, and the testing set. The purpose of the training set is to enable the system to discern the underlying patterns and relationships between the input data and the corresponding desired outputs. This process facilitates the establishment of a functional mapping between the input variables and the expected outcomes.

In this study, the appropriate ANN structure was determined by developing multiple networks to predict the behavior of the grey relational grade, as shown in Table 11. Validation is crucial in ensuring the network has been properly trained. Insufficient training of ANNs can lead to inefficiency and inaccurate predictions. The variation values in Table 11 demonstrate that the ANN

can accurately predict the grey relational grade. Furthermore, the ANN results show that the grade values are very close, with minimal variation between the grade values obtained from grey relation analysis and the predicted grade values. This indicates that the optimal parameters confirmed by grey relation analysis significantly improved the material removal rate and machining depth. The regression plot for the entire dataset of grey relational grade is depicted in Figure 10.

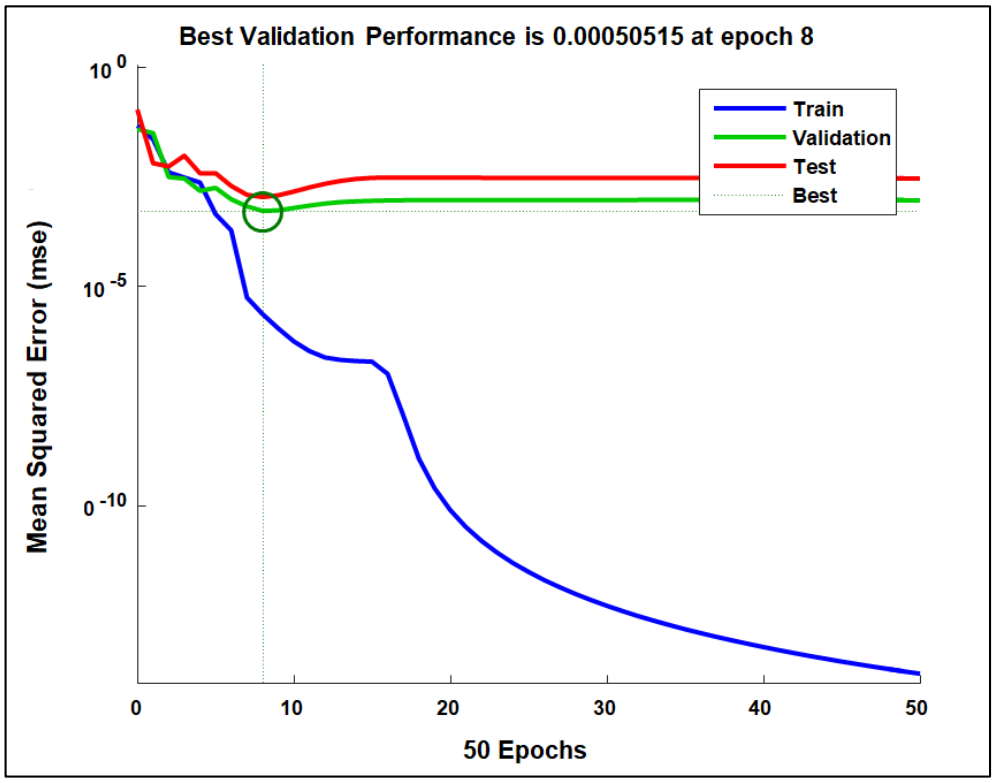

Figure 9: Training and test performance graph

Table 11: Data for training and testing of the ANN

Current (A)	SOD (mm)	Gap (mm)	electrolyte	Concentration (%)	grade	ANN	variation
20	0.1	30	1	0.05	0.367555	0.36748	7.4878E-05
20	0.2	40	2	0.1	0.35921	0.36838	-0.0091698
20	0.3	50	3	0.15	0.416319	0.41714	-0.0008214
20	0.4	60	4	0.2	0.468838	0.46947	-0.0006322
20	0.5	70	5	0.25	0.496791	0.54406	-0.0472692
35	0.1	40	3	0.2	0.625566	0.62396	0.00160635
35	0.2	50	4	0.25	0.72337	0.72137	0.00199965
35	0.3	60	5	0.05	0.34785	0.33991	0.00793991
35	0.4	70	1	0.1	0.333333	0.3611	-0.0277667
35	0.5	30	2	0.15	0.416261	0.41625	1.0656E-05
50	0.1	50	5	0.1	0.494602	0.49482	-0.000218
50	0.2	60	1	0.15	0.483376	0.48564	-0.0022639
50	0.3	70	2	0.2	0.485794	0.52344	-0.0376459
50	0.4	30	3	0.25	0.737312	0.73472	0.00259187
50	0.5	40	4	0.05	0.391961	0.39228	-0.0003188
65	0.1	60	2	0.25	0.7906	0.79039	0.00020957
65	0.2	70	3	0.05	0.432927	0.45572	-0.0227934
65	0.3	30	4	0.1	0.566374	0.55351	0.01286391
65	0.4	40	5	0.15	0.543697	0.5433	0.00039723
65	0.5	50	1	0.2	0.5409	0.54286	-0.0019601
80	0.1	70	4	0.15	0.714122	0.71516	-0.0010375
80	0.2	30	5	0.2	0.947409	0.97904	-0.0316309
80	0.3	40	1	0.25	1	0.99917	0.00083
80	0.4	50	2	0.05	0.430251	0.43148	-0.0012287
80	0.5	60	3	0.1	0.49036	0.49372	-0.0033602

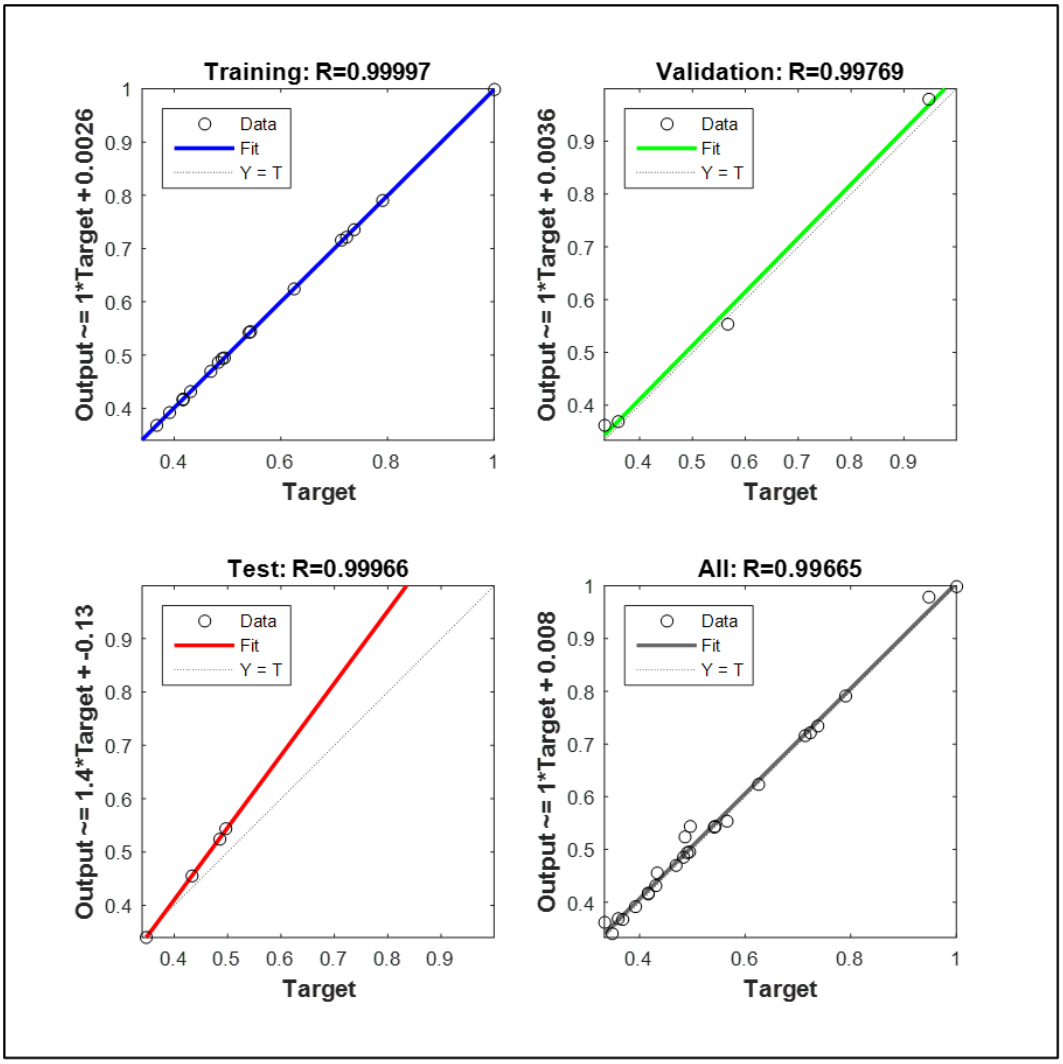

Figure 10: The plot of all data regression for the data set of grey relation grade

5.4 Surface Topography of The Machined Workpiece

The roughness characteristic results from numerous craters overlapping and the shape of these craters is influenced by process variables and changes in material properties [36]. Scanning Electron Microscopy (SEM) analysis was performed to assess the machined WC-Co composite material's surface quality. Various magnifications were used to capture the surface topography of different machined samples, allowing for observing surface features. Figure 11a illustrates that the surface exhibits shallow craters and small debris, particularly prominent at higher input process parameter levels. These craters formed due to the extraction of non-conductive particles and the presence of ceramic particles protruding on the machined surface [37]. Also, microcracks appeared on the machined surfaces of tungsten carbide workpieces during experiments 13 and 18, as revealed in Figures 11 b and c. Because of their lower melting point, the cobalt particles melt and separate from the tungsten carbide surface [6].

Machining tungsten carbide using ECDM improves surface quality, featuring a finer finish with minimal microcracks and shallow craters. These surface attributes result from the high temperatures generated by the sparks during the process. The elevated temperatures cause the work material to melt and even evaporate rapidly due to the cooling effect of the flushing electrolyte, which helps minimize microcracks. This combination of electrochemical material dissolution and the high-temperature spark effect results in fewer microcracks than observed in the EDM process. When observed at a magnification of 1500x, surface characteristics in EDM, such as craters, cracks, and re-deposited debris, become clearly visible [37]. These imperfections are directly linked to the energy discharges during the process [38].

The electrochemical discharge method for machining tungsten carbide produces a finer surface finish than electrical discharge machining (EDM). This study measured the average surface roughness achieved with Electrochemical Discharge Machining (ECDM) of tungsten at 0.9275 µm. In contrast, for Electrical Discharge Machining (EDM) of tungsten carbide, the lowest average surface roughness found was 2.214 µm [9].

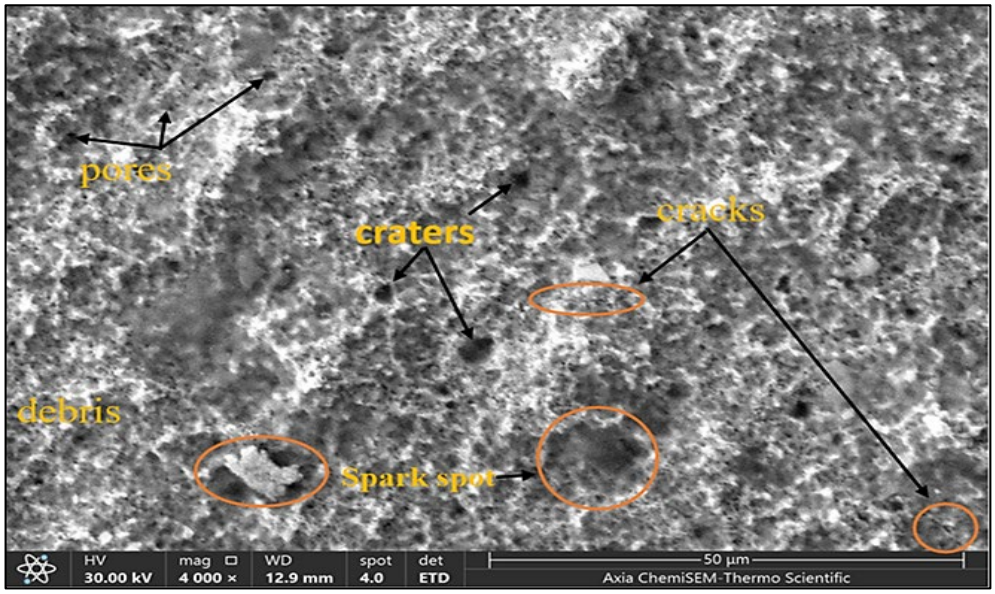

(a)

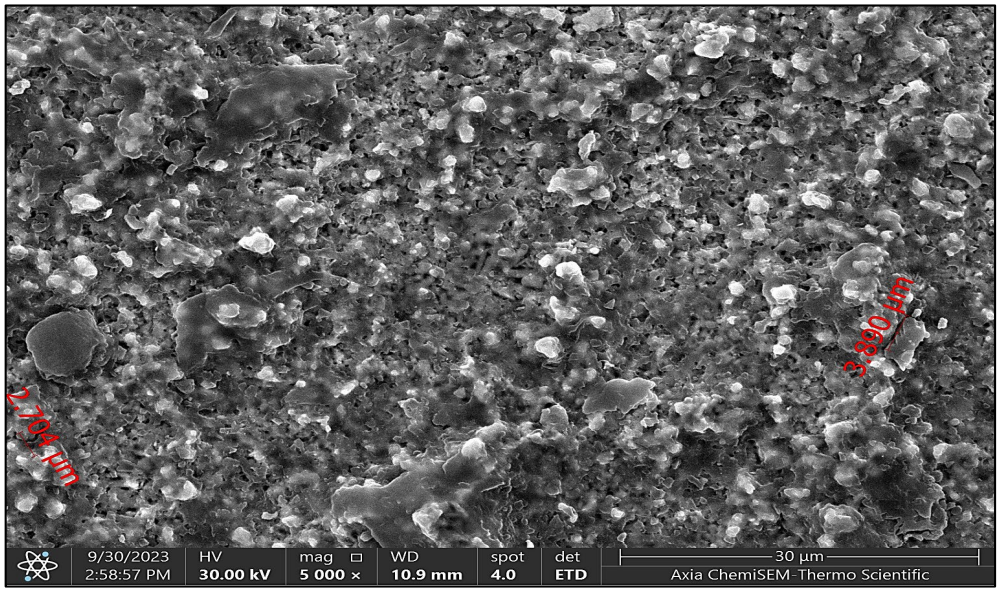

(b)

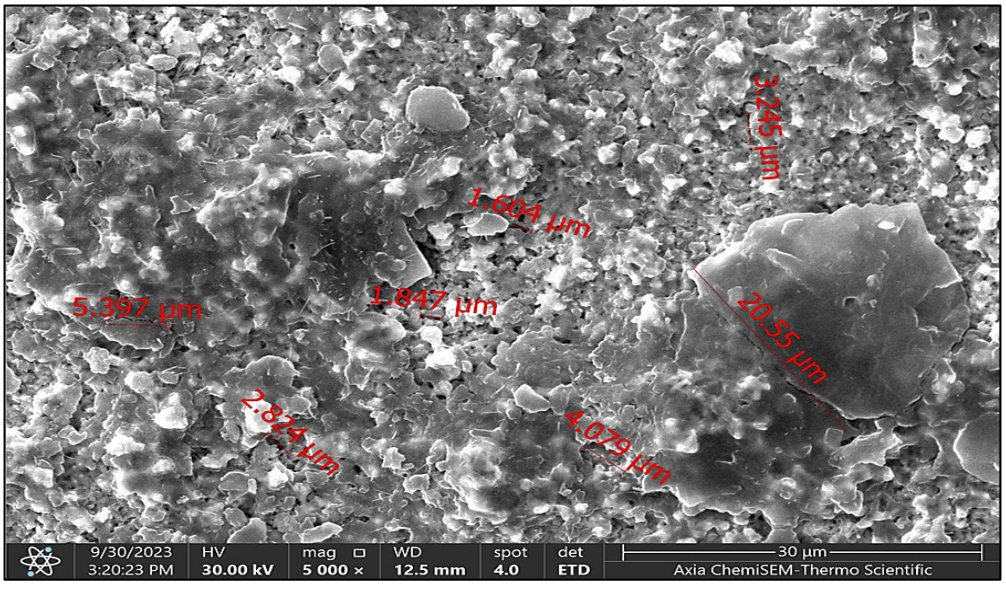

(c)

Figure 11: a) Shallow craters and small debris on the machined surface b) Microcracks on the machined surface of sample 13 c) Microcracks on the machined surface of sample 18

5.5 Compositions of The Machined Workpiece Surface

The chemical composition of tungsten carbide before and after machining copper electrodes was assessed using energy-dispersive X-ray spectroscopy (EDS). Figures 12 and 13 correspond to the EDS results presented in Tables 1 and 2, respectively. In Figure 12, peaks for tungsten, carbon, and other chemical elements are clearly visible on Tungsten carbide workpiece before ECDM machining. Furthermore, Figure 13 highlights the copper peak as the most prominent.

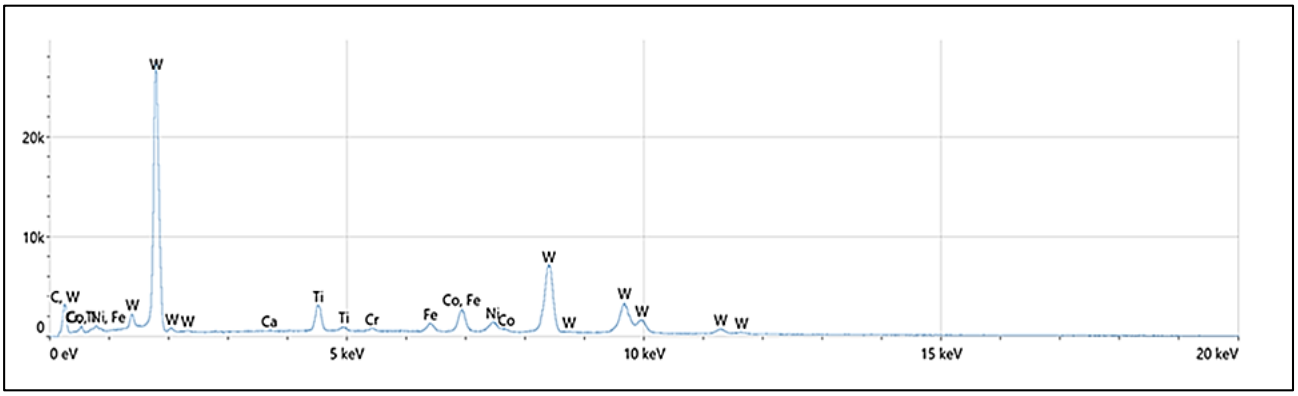

Figure 12: EDS chart of tungsten carbide workpiece before machining

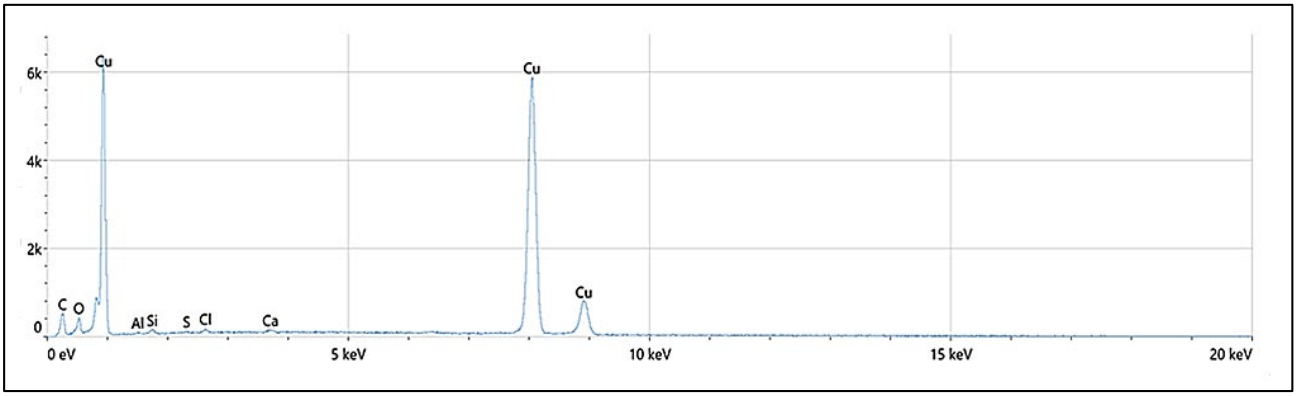

Figure 13: EDS chart of copper electrode

The specimens underwent Energy Dispersive X-ray (EDX) analysis to explore how the structure and composition changed during the ECDM process. Figure 14 displays the SEM EDX analysis of the affected surfaces, conducted at an accelerating voltage of 20 kV. The EDX analysis revealed the presence of residual aluminum (Al) in the tungsten carbide composite sample. This occurrence was attributed to the electrochemical dissolution of the aluminum fixture employed to secure the workpiece during the experiments. Furthermore, the EDX results indicated the presence of carbon (C) and oxygen (O) in the tungsten carbide composite sample. The oxygen presence in the tungsten carbide composite sample likely resulted from oxidation induced by the high temperatures in the process. Notably, carbon (C) and oxygen (O) were also observed in the tungsten carbide composite sample when it was machined using the EDM process [36,38]. In the electrical discharge machining (EDM) of tungsten carbide material, the recast layer displayed tungsten (W) and carbon (C) with a minimal presence of cobalt (Co). It was noted that during EDM, cobalt could reach its evaporation temperature before the tungsten carbide (WC) particles melted. Consequently, this process can lead to the forming of a cobalt-free region within the EDMed material [40].

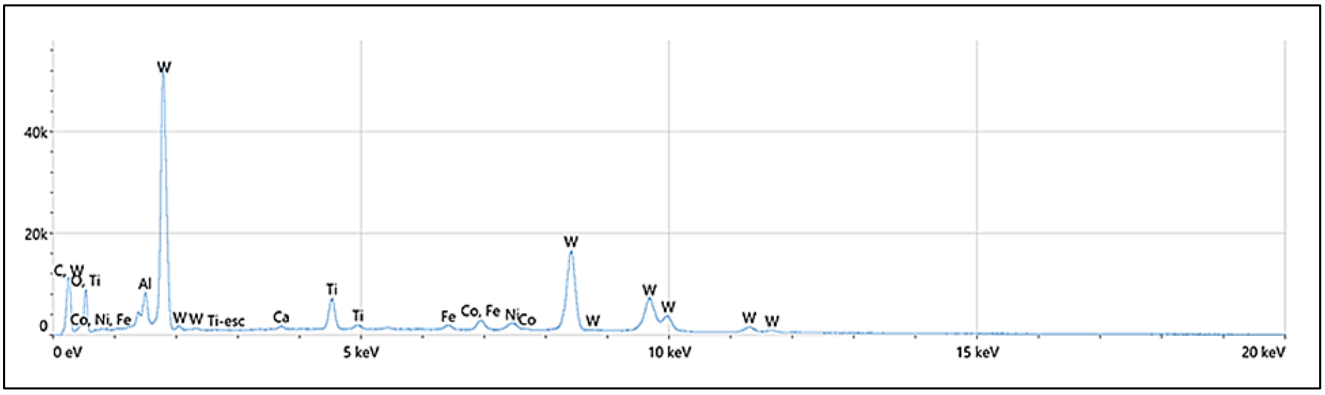

Figure 14: EDX analysis result of tungsten carbide sample after ECDM

6. Conclusion

This work investigates optimizing machining parameters and their impact on Material Removal Rate (MRR) and Machining Depth (MD) in ECDM operations. The significance of the machining parameters on MRR and MD is evaluated through grey relation analysis. The grey relation grade was predicted using ANN. Based on the findings, the following conclusions can be drawn:

1) Using orthogonal arrays with GRA and ANN to optimize ECDM process parameters for fabricating tungsten carbide materials with multiple performance characteristics has proven effective, simplifying the optimization process through this approach.
2) The material removal rate and machining depth of tungsten carbide were successfully improved using grey relation analysis within the framework of the Taguchi technique.
3) According to the analysis of variance, the electrolyte concentration contributes 50.55% to the material removal rate and machining depth, while the current value has a 31.32% impact.
4) Current (80 A), SOD (0.1 mm), gap (30 mm), electrolyte concentration (25%), and electrolyte type (KCl +KOH) were shown to be the best combinations of ECDM process parameters for machining tungsten carbide based on grade relation analysis and artificial neural network.
5) It has been observed that the predicted GRG by artificial neural network aligns well with the mathematically obtained results, indicating the optimal process parameters for ECDM of tungsten carbides.
6) Observations under the SEM microscope show the presence of shallow craters, limited microcracks, and small re-deposited melt particles on the machined surfaces. These findings help account for the smooth surfaces attained after the ECD process. The average surface roughness recorded in this study for Electrochemical Discharge Machining (ECDM) of tungsten measures 0.9275 µm.
7) Utilizing EDX analysis, remaining traces of aluminum (Al) were identified within the tungsten carbide composite sample. Additionally, the analysis revealed the presence of carbon (C) and oxygen (O) in the tungsten carbide composite sample. The likely reason for the oxygen presence in the tungsten carbide composite sample is the result of oxidation caused by the elevated temperatures involved in the process.

Acknowledgments

The authors would like to thank the University of Technology- Iraq for their support in completing this research work.

Author contributions

Conceptualization,V. Najm,T. Abbas and Sh. Aghdeab; writing—review and editing, V. Najm,T. Abbas, and Sh. Aghdeab; All authors have read and agreed to the published version of the manuscript.

Funding

This research received no specific grant from any funding agency in the public, commercial, or not-for-profit sectors.

Data availability statement

The data that support the findings of this study are available on request from the corresponding author.

Conflicts of interest

The authors declare that there is no conflict of interest.

References

[1] W. Tang, X. Kang, W. Zhao, J. Qian, and B. Lauwers, Discharge Characteristics in Electrochemical Discharge Machining of Ceramic-coated Ni-superalloy, Procedia CIRP, 95 (737–742) 2020. https://doi.org/10.1016/j.procir.2020.02.307

[2] V. V. Vani, S.K.Chak, A Review on Electro Chemical Discharge Machining (Ecdm) of Al-Based Metal Matrix Composites (Mmc), Int.J. Mech. Prod. Eng., 4 (2016) 128-134.

[3] T. K. K. R. Mediliyegedara, A. K. M. De Silva, D. K. Harrison, and J. A. McGeough, An intelligent pulse classification system for electro-chemical discharge machining (ECDM) - A preliminary study, J. Mater. Process. Technol., 149 (2004) 499–503. https://doi.org/10.1016/j.jmatprotec.2004.04.002

[4] S. K. Chak, Electro Chemical Discharge Machining: Process Capabilities, Int. J. Mech. Prod. Eng., 4 (2016) 135–146.

[5] A. P. Study, Synthesis and Sintering of Tungsten and Titanium Carbide: A Parametric Study, 2022.

[6] P. Janmanee and S. Kumjing, A study of tungsten carbide surfaces during the electrical discharge machining using artificial neural network model, Int. J. Appl. Eng. Res., 12 (2017) 3214–3227.

[7] A. Fadhil Ibrahim, M. Adel Abdullah, and S. Kadhim Ghazi, Prediction of Surface Roughness and Material Removal Rate for 7024 AL-Alloy in EDM Process, Eng. Technol. J., 34 (2016) 2796–2804. https://doi.org/10.30684/etj.34.15a.2

[8] S. K. Shather, Prediction of Particle size and Material Removal Rate of zinc oxide, February, 2020.

[9] G. Kumar, J. S. Tiwana, and A. Singla, Optimization of the machining parameters for EDM wire cutting of Tungsten Carbide, MATEC Web Conf., 57 (2016)1–4. https://doi.org/10.1051/matecconf/20165703006

[10] A. Equbal and A. K. Sood, Electrical Discharge Machining: An Overview on Various Areas of Research, Manuf. Ind. Eng., 13 (2014) 1-6 . https://doi.org/10.12776/MIE.V13I1-2.339

[11] P. K. Shrivastava and A. K. Dubey, Electrical discharge machining-based hybrid machining processes: A review, Proc. Inst. Mech. Eng. Part B J. Eng. Manuf., 228 (2014)799–825. https://doi.org/10.1177/0954405413508939

[12] S. A. Khan et al., A detailed machinability assessment of dc53 steel for die and mold industry through wire electric discharge machining, Metals (Basel) 11(2021). https://doi.org/10.3390/met11050816

[13] M. U. Farooq, M. P. Mughal, N. Ahmed, N. A. Mufti, A. M. Al-Ahmari, and Y. He, On the investigation of surface integrity of Ti6Al4V ELI using si-mixed electric discharge machining, Materials (Basel)., 13 (2020) 1549. https://doi.org/10.3390/ma13071549

[14] M. Rafaqat et al., Hole-Making in D2-Grade Steel Tool by Electric-Discharge Machining through Non-Conventional Electrodes, Processes, 10 (1–24) 2022. https://doi.org/10.3390/pr10081553

[15] M. U. Farooq et al., A Novel Flushing Mechanism to Minimize Roughness and Dimensional Errors during Wire Electric Discharge Machining of Complex Profiles on Inconel 718, Materials (Basel)., 15 (2022). https://doi.org/10.3390/ma15207330

[16] N. Shibuya, Y. Ito, and W. Natsu, Electrochemical machining of tungsten carbide alloy micro-pin with NaNO3 solution, Int. J. Precis. Eng. Manuf., 13 (2012) 2075–2078 2. https://doi.org/10.1007/s12541-012-0273-2

[17] D. Zander, A. Schupp, O. Beyss, B. Rommes, and A. Klink, Oxide formation during transpassive material removal of martensitic 42CrMo4 steel by electrochemical machining, Materials (Basel)., 14 (2021) 1–16. https://doi.org/10.3390/ma14020402

[18] hassan Abdel-Gawad El-Hofy, advanced machining processes n0ntraditional and hybrid machining processes, 4,2005.

[19] S. S. H and B. R. I, Parametric optimization of Electro Chemical Spark Machining using Taguchi based Grey Relational Analysis, IOSR J. Mech. Civ. Eng., (2012) 46–52.

[20] M. Durairaj, D. Sudharsun, and N. Swamynathan, Analysis of process parameters in wire EDM with stainless steel using single objective Taguchi method and multi objective grey relational grade, Procedia Eng., 64 (2013) 868–877. https://doi.org/10.1016/j.proeng.2013.09.163

[21] N. Manikandan, S. Kumanan, and C. Sathiyanarayanan, Engineering Science and Technology , an International Journal Multiple performance optimization of electrochemical drilling of Inconel 625 using Taguchi based Grey Relational Analysis, Eng. Sci. Technol. an Int. J., 20 (2017) 662–671. https://doi.org/10.1016/j.jestch.2016.12.002

[22] N. Kumar, H. Bishwakarma, P. Sharma, P. K. Singh, and A. K. Das, Optimization of process parameters in micro-electrochemical discharge machining by using grey relational analysis, Mater. Sci. Forum, 978 (2020) 121–132. https://doi.org/10.4028/www.scientific.net/MSF.978.121

[23] P. Pawar, A. Kumar, and R. Ballav, Grey relational analysis optimization of input parameters for electrochemical discharge drilling of silicon carbide by gunmetal tool electrode, Ann. Chim. Sci. des Mater., 44 (2020) 239–249. https://doi.org/10.18280/acsm.440402

[24] S. A. Hammood, Optimization of Cutting Parameters for Milling Process of (4032) Al-Alloy using Taguchi-Based Grey Relational Analysis, 17 (2021) 1–12.

[25] N. Tamiloli, J. V.enkatesan, B.V. Ramnath, A grey-fuzzy modeling for evaluating surface roughness and material removal rate of coated end milling insert, Measurement, 84 (2016) 68–82. https://doi.org/10.1016/j.measurement.2016.02.008

[26] L. Paul and S. S. Hiremath, Evaluation of Process Parameters of ECDM Using Grey Relational Analysis, Procedia Mater. Sci., 5 (2014) 2273–2282. https://doi.org/10.1016/j.mspro.2014.07.446

[27] A. N. Haq, P. Marimuthu, and R. Jeyapaul, Multi response optimization of machining parameters of drilling Al/SiC metal matrix composite using grey relational analysis in the Taguchi method, Int. J. Adv. Manuf. Technol., 37 (2008) 250–255. https://doi.org/10.1007/s00170-007-0981-4

[28] V. Rajput, S. S. Pundir, M. Goud, and N. M. Suri, Multi-Response Optimization of ECDM Parameters for Silica (Quartz) Using Grey Relational Analysis, Silicon, 13 (2021) 1619–1640. https://doi.org/10.1007/s12633-020-00538-7

[29] M. U. Farooq, S. Anwar, and A. Hurairah, Reducing micro-machining errors during electric discharge machining of titanium alloy using nonionic liquids, Mater. Manuf. Process., 38 (2023) 1–16. https://doi.org/10.1080/10426914.2023.2236199

[30] J. W. Liu, T. M. Yue, and Z. N. Guo, An analysis of the discharge mechanism in electrochemical discharge machining of particulate reinforced metal matrix composites, Int. J. Mach. Tools Manuf., 50 (2010) 86–96. https://doi.org/10.1016/j.ijmachtools.2009.09.004

[31] K. R. Kolhekar and M. Sundaram, Study of gas film characterization and its effect in electrochemical discharge machining, Precis. Eng., 53 (2018) 203–211. https://doi.org/10.1016/j.precisioneng.2018.04.002

[32] T. GENG and Z. XU, Electrochemical discharge machining for fabricating holes in conductive materials: A review, J. Adv. Manuf. Sci. Technol., 1(2021) 2021006. https://doi.org/10.51393/j.jamst.2021006

[33] S. G. Dileepkumar, K. N. Bharath, B. C. Naveen, and A. Kumar, A Study of Response Parameters during ECDM on Quartz Material, IOP Conf. Ser. Mater. Sci. Eng., 925 ((2020). https://doi.org/10.1088/1757-899X/925/1/012053

[34] V. Sharma and S. Kumar, Experimental research to Optimize Process Parameters in Machining of Non Conducting Material with hybrid non conconventional machining, Int. J. Trend Sci. Res. Dev., 1(2017) . https://doi.org/10.31142/ijtsrd84

[35] D. Kumar Kasdekar, V. Parashar, and C. Arya, Artificial neural network models for the prediction of MRR in Electro-chemical machining, Mater. Today Proc., 5 (2018) 772–779. https://doi.org/10.1016/j.matpr.2017.11.146

[36] M. P. Mughal et al., Surface modification for osseointegration of Ti6Al4V ELI using powder mixed sinking EDM, J. Mech. Behav. Biomed. Mater., 113 (2021) 104145. https://doi.org/10.1016/j.jmbbm.2020.104145

[37] P. Kumar and P. Rawat, Investigating the Effects of Wire Electric Discharge Machining Parameters on MRR and Surface Integrity in Machining of Tungsten Carbide Cobalt (WC-24% Co) Composite Material, 2 (2015) 29–35.

[38] M. U. Farooq et al., Curved profiles machining of Ti6Al4V alloy through WEDM: investigations on geometrical errors, J. Mater. Res. Technol., 9 (2020) 16186–16201. https://doi.org/10.1016/j.jmrt.2020.11.067

[39] S. H. Lee and X. Li, Study of the surface integrity of the machined workpiece in the EDM of tungsten carbide, J. Mater. Process. Technol., 139 (2003) 315–321. https://doi.org/10.1016/S0924-0136(03)00547-8

[40] M. B. Toparli, Wire-EDM Cutting Strategies of WC-Co Hardmetals : Effect of Number of EDM Pass on Surface Integrity Wire-EDM Cutting Strategies of WC-Co Hardmetals. (2022) 1–18. https://doi.org/10.21203/rs.3.rs-1664872/v1